A compliant soft-actuator laterotactile display

Espen Knoop[1,2], **Jonathan Rossiter**[1,2]

[1]Department of Engineering Mathematics, University of Bristol, University Walk, Bristol BS8 1TR, UK

[2]Bristol Robotics Laboratory, T Block, Frenchay Campus, Coldharbour Lane, Bristol, BS16 1QY, UK

E-mail: espen.knoop@bristol.ac.uk

Abstract. Humans are extremely adept at eliciting useful information through touch, and the tactile domain has huge potential for handheld and wearable electronic devices. Smart materials may be central to exploiting this potential. The skin is highly sensitive to laterotactile stimulation, where tactile elements move laterally against the skin, and this modality is well suited for wearable devices. Wearable devices should be soft and compliant, in order to move with the user and be comfortable.

We present and characterise a laterotactile display using soft and compliant Dielectric Elastomer Actuators (DEAs). We carry out an initial psychophysical study to determine the absolute sensitivity threshold of laterotactile stimulation, and find that at low frequencies sensitivity is higher than for normal tactile stimulation. Our results suggest that the mechanoreceptors close to the skin surface (SA1, FA1) have improved sensitivity to laterotactile stimulation.

We believe our results lay the foundation for a range of new soft robotic human interface devices using smart materials.

Keywords: Tactile display, Laterotactile stimulation, Dielectric elastomer actuator, Electroactive polymer, Compliant mechanism.

Submitted to: *Smart Mater. Struct.*

1. Introduction

Humans are extremely adept at interacting through, and eliciting useful information from, the sense of touch. However when interacting with modern technology such as computers and smartphones only limited information is presented through the tactile domain. This is due to limitations of current actuator technology. A sophisticated tactile display would require a large array of actuators to create a tactile illusion in the skin of the user, which is currently not economically feasible.

For wearable devices such as smart watches, the tactile domain would seem ideal for communication with the user. The sense of touch is inherently more intimate and personal than the other senses; it relies on physical contact between the sender and the receiver. It is also distributed over the entire body rather than being sensed at a particular location. If a tactile device also featured tactile sensing, two-way tactile communication with the user becomes possible. As an augmentation of the user experience, tactile communication would enrich and enhance communication.

A wearable device would have to be bio-compatible and bio-integrative; it would have to be compliant in order to move with the user and conform to the skin.

Tactile displays can be static, e.g. in relief maps or Braille, where the user actively explores the tactile stimuli. Alternatively, dynamic tactile displays such as the Optacon [1] convey tactile information while resting against the skin of the user. In a wearable device, dynamic tactile information would be required.

In this paper, we develop a compliant dynamic tactile display, suitable for use as a wearable device. We characterise the display, and carry out a preliminary psychophysical study to assess the performance.

1.1. Laterotactile stimulation

Humans are sensitive to stimuli from DC up to ∼400 Hz [2]. In the glabrous skin of the hand, this is mediated through 4 mechanoreceptors and afferents as shown in Fig. 1 (a). The mechanoreceptors are sensitive to different mechanical responses and have different frequency responses [2, 3, 4]. The spatial sensitivity of the fingertip for static stimuli is ∼1 mm [5].

Studies [6, 7, 8] have found that humans are highly sensitive to shear deformations of the skin where contactors moving laterally against the surface of the skin create regions of compressive and tensile strain. This is different from normal tactile stimulation which has been investigated in tactile displays [9, 10, 11] and characterised in psychophysical and physiological studies [3, 4, 12]. In many cases the perceived sensations from laterotactile stimulation are indistinguishable from normal tactile stimulation [6, 7].

Kikuuwe *et al* [6, 13] created the Tactile Contact Lens (TCL), a passive device converting surface undulations into laterotactile stimulation through an array of pins. In an object localisation task, where users were required to locate a small paper disk placed under a rubber sheet, the TCL was found to improve performance. This suggests that humans are very sensitive to shear stimuli. Moreover, the perceived sensation created by

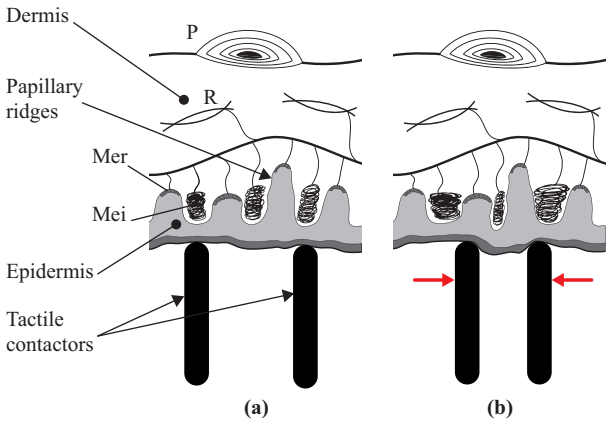

Figure 1. Diagram of the glabrous skin structure. The epidermis (outer skin) is shown in gray, and the mechanoreceptors have been labelled. *Mei*: Meissner Corpuscle, FA1 afferent; *Mer*: Merkel Cells, SA1 afferent; *R*: Ruffini Ending, SA2 afferent; *P*: Pacinian Corpuscle, FA2 afferent. The skin is shown at rest (a) and with our hypothesised effect of a laterotactile stimulus (b). It can be seen that the Meissner Corpuscles are stretched and compressed, and the Merkel Cells will also be stimulated.

the TCL is that of normal surface undulations—it doesn't feel like the pins are moving laterally.

Laterotactile stimulation has been investigated in [7, 14, 8], among others, using an array of piezoelectric cantilever actuators stimulating the fingerpad. They are able to create sophisticated stimuli, and note that the tactile display is capable of 'a number of curious sensations' including pulses, travelling waves and random 'noise'.

Hayward *et al* [8] show that for a tactile display device with sufficient spatial resolution there is equivalence between normal and shear stimulation; the same strain distributions in the skin can be created with purely normal stimulation or with purely shear stimulation. This means that a tactile device operating in one of those modalities will be able to create any tactile sensation.

Fig. 1 (a) shows the structure of the glabrous skin of the fingertip. The inside of the epidermis has papillary ridges innervated by Merkel cells and Meissner corpuscles as shown. The epidermis (outer skin) is 1,000–10,000 times harder than the dermis (inner skin) and subcutaneous tissue [15].

We hypothesise that laterotactile stimulation strains the regions of the epidermis between the papillary ridges, thus displacing them as indicated in Fig. 1 (b). This suggests that it is well suited for stimulating the SA1 and FA1 afferents, and agrees with the hypothesis presented by [16]. For the SA2 and FA2 afferents embedded deeper in the tissue, it would seem that the nature of the tactile stimuli (lateral or normal) is of less significance.

The design requirements and psychophysical properties of laterotactile stimulation are not well understood. Some characterisation of the tactile sensitivity has been carried out [17, 18, 19, 20] however the psychophysical space remains to be explored. We estimate that TCL presented in [6], with a pin spacing of 1.5 mm, undergoes lateral

displacements on the order of 50 μm that can be clearly detected. We assume this is primarily stimulating the SA mechanoreceptors: a feature size of 5.5 mm with a scanning speed of 20 mm/s [21] would suggest frequencies on the order of 4 Hz. It would seem that the amplitude required for detection will be a function of the stimulus frequency as well as the spacing between pins.

1.2. Soft actuators for compliant tactile displays

The laterotactile displays discussed above use piezoelectric materials [7, 14] and electric motors [18] for actuation. Piezoelectric materials generate small intrinsic strains that require mechanical amplification such as cantilever beams to generate tactile output [22, 14]. To create inherently compliant tactile displays suited for wearable devices, we require compliance in both the actuator and the device structure as a whole. By compliance, we mean that the tactile elements in contact with the user's skin can be elastically displaced while tactile information is being presented, to allow for the user to move naturally.

Pneumatic actuation of an entirely soft structure is possible [23], however this requires an external air supply and each actuator requires an external controller. Consequently this approach does not scale to large arrays of actuators.

Electroactive Polymers (EAPs) are a class of actuators that change shape when stimulated electrically and have a number of desirable properties for tactile displays. In particular, Dielectric Elastomer Actuators (DEAs) appear to be well suited for this application [24]. When an electric field is applied across an elastomer membrane, the resultant electrostatic stress squeezes the membrane and causes it to undergo areal expansion (Fig. 2). The electrostatic stress P acting through the thickness of the membrane is given by

$$P = \varepsilon_0 \varepsilon_r \frac{V^2}{d^2} \tag{1}$$

where ε_0 is the permittivity of free space, ε_r is the relative permittivity of the dielectric, V is the voltage and d is the thickness of the membrane. DEAs require high electric fields of $\sim$100 V/μm, so the required voltage is proportional to the thickness of the membrane. With state-of-the-art fabrication techniques, voltages up to the order of 1 kV are typically required [25].

The inherent compliance, high power density, low mechanical complexity and large strains of DEAs makes them very attractive for this application area. Additionally, DEAs can simultaneously be used for sensing as well as actuation [26]. A tactile display with DEAs could therefore also function as a tactile sensor, enabling true 2-way tactile communication.

It has been argued that electroactive polymers hold the key to the 'holy braille' of virtual Braille displays, a low-cost full-page refreshable braille display. There are a number of examples of DEA-actuated tactile displays [27, 28, 29, 30, 31, 32, 33, 34] however they all feature elements moving perpendicular to the skin and generating

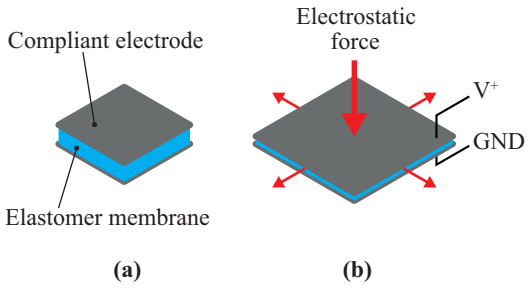

Figure 2. Operating principle of a Dielectric Elastomer Actuator (DEA). The DEA rest state is shown in (a). When a voltage is applied across an elastomer membrane, the electrostatic force squeezes the membrane and causes it to expand in area (b).

normal forces. We presented a first prototype of a DEA-actuated laterotactile display in [35]. Here we presented the mechanism used in this paper, and demonstrated that the prototype display could generate clearly noticeable tactile sensations.

DEAs have started to make the transition from research to industry, notably being used in the mass-produced *ViviTouch* technology by *Artificial Muscle, Inc.* for haptic feedback. Long lifetimes at extremely high strains are currently difficult to achieve [25], but significant progress is currently being made in this area.

2. Development

A mechanism is required to convert the strain of the DEA into useful tactile output. The in-plane areal strains of the DEA would seem particularly well suited for laterotactile stimulation. In particular, we require a mechanism that can be scaled up to large arrays and is passively compliant.

Conn *et al* [36, 37] discusses different designs of cone DEAs. Only individual cones are considered, with the DEA membrane rigidly supported for each unit. A tactile display with an array of cone actuators would allow for independent control of each pin in the device, and would be readily realisable. However, this would require rigid support of the DEA membrane around each pin in the device.

Our proposed mechanism for DEA laterotactile stimulation, presented in Fig. 3, uses a simplified actuator structure. Rigid pins are attached to a continuous surface with a spherical joint. A continuous DEA membrane is attached to the bottom of the pins, with a pattern of electrodes. Actuation of an element of the DEA causes it to expand in area, moving the adjacent pins. The user rests his finger against the top of the pins and DEA actuation causes local compression of the fingertip skin.

The hinged structure allows for tuning of the force/displacement output of the device by changing the relative length of the top and bottom elements of the pins (Fig. 4 (a): b and c) to be optimal given the stiffness of the DEA membrane and the fingertip of the user. By actuating the bottom of the pins, the high-voltage DEA can be placed underneath the device surface and further away from the user. For integration into consumer products, this would seem to be a clear advantage. The hinge also takes

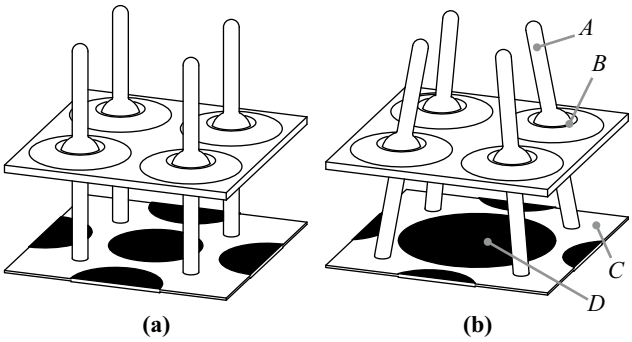

Figure 3. Our proposed mechanism for laterotactile stimulation. Rigid pins (A) are attached to a surface with compliant spherical joints (B). A DEA membrane (C) is attached to the bottom of the pins, and the user's finger rests against the top of the pins. The device at rest is shown in (a). Actuation of a DEA element, shown in black (D), causes it to expand in area which causes compression at the fingertip (b).

up the normal force from the user touching the device.

A soft and compliant tactile display will deform and move with the user, so that it is the relative movement of adjacent pins rather than the movement of single pins that will create strain distributions across the fingertip of the user. Our design couples the movement of adjacent pins because actuation of any DEA element results in relative movement of surrounding pins.

For a large rectangular array of pins and DEA elements, the number of pins will be equal to the number of DEA elements. Each pin has 2 degrees of freedom, so the system of pins is not fully controllable. Moreover, each pin is between 4 DEA elements so the system is heavily coupled. However, if we instead consider the output to be the areal strains on the skin surface then for small displacements the system becomes both controllable and decoupled as each DEA element applies areal strains to the region of skin directly above it. Simultaneous actuation of multiple adjacent DEA elements will create more complex output. Areal expansion of one element will rely on the strain in the DEA membrane being taken up by the surrounding elements, so that any actuation pattern would be expected to require each actuated DEA element to be adjacent to at least one passive (non-actuated) DEA element.

We fabricated a prototype Laterotactile Pin Display (LPD) device using a multi-material 3D printer (Objet260 Connex, Stratasys Ltd.) printing rigid and compliant materials. Here the pins were made from rigid material and the spherical joints were implemented as soft elastomer hinges. For simplified characterisation, our design featured a rigid frame, but the design can readily be modified to have a compliant frame. The DEA membrane was attached after printing. With advances in 3D printing technology the DEA membrane could be printed as an integral part of the structure as demonstrated by Rossiter *et al* [38]. The use of a single continuous DEA membrane rather than individual DEAs for each pins means that large arrays and sheet materials could be readily fabricated in this way.

In this paper we study a single tactile display element, with four pins and a single

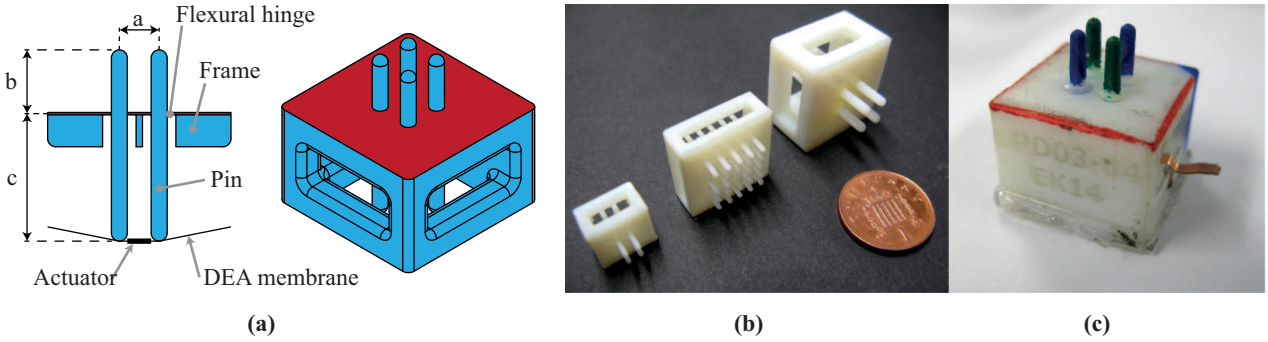

Figure 4. LPD prototypes. (a): Section view through flexural hinge, as well as isometric view of device. Soft material is shown in red, and rigid material is shown in blue. For the characterised prototype, a=5 mm, b=8 mm and c=16 mm. The DEA membrane (black) is attached to the bottom of the pins, with an electrode element (black) between the pins. (b): The different versions of LPD. The left and centre devices have pin spacings of 2.5 mm, and the rightmost one has a pin spacing of 5 mm. The rightmost one has been used for further study here. (c): Close-up view of the characterised device with 5 mm pin spacing . The pins have been coloured for motion-tracking.

DEA element, and a pin spacing of 5 mm. Results from a single element will also apply to large arrays. A CAD drawing of the characterised LPD prototype is presented in Fig. 4 (a), and the 3D-printed prototypes are shown in Fig. 4 (b) and (c) and. We have also demonstrated that with our presented design and manufacturing method we can make devices with 2.5 mm pin spacings that would be capable of producing sophisticated tactile output.

We used a single-layer acrylic dielectric elastomer membrane (VHB 4905, 3M), biaxially pre-strained to 1600 % area strain. This gives an estimated elastomer thickness of 31 μm. Carbon grease electrodes (MG chemicals) were brushed on using a stencil.

3. Characterisation

We have carried out tests to determine the stiffness and force output of the LPD, the bandwidth, the free displacement and the displacement with a finger resting on the unit.

Experiments were controlled from a PC running MATLAB, with a data acquisition board (NI-PCI6229, National Instruments). A power amplifier (HA-151A, Hokuto Denko) and a DC-DC converter (F121, Emco) were used to drive the DEA. The voltage across the DEA was measured using the data acquisition board after stepping it down by a factor of 1000 through a potential divider.

Fig. 5 shows an annotated diagram of the LPD with numbered pins and directions u (side view), v (bottom view) and w (corner view) indicated. We define the pin displacement δ_i to be the absolute displacement of the top of the pin, as labelled, and A to be the area enclosed by the tops of the pins as indicated.

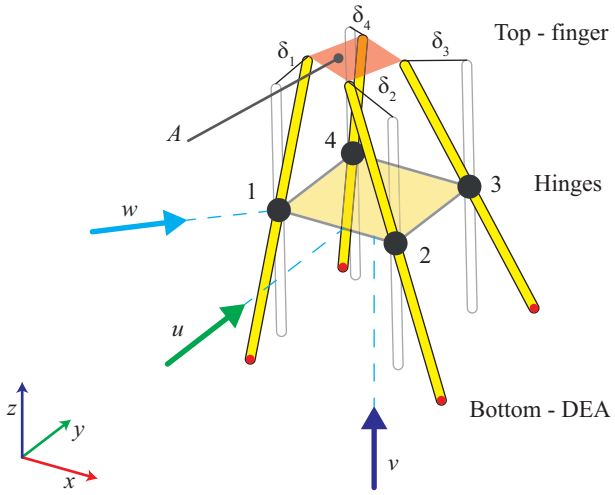

Figure 5. Schematic diagram of LPD mechanism, with pins numbered 1–4 and directions u (side view), v (bottom view) and w (corner view). The displacment of each pin i has been labelled δ_i. Also labelled is A, the area enclosed by the tops of the pins.

3.1. Force and stiffness

For force measurements, load cells (LV5S and LMA-A-10N, Kyowa) were used together with an amplifier (DPM-912B, Kyowa). Position was measured with a Laser Displacement Meter (LK-G152 and LK-GD500, Keyence).

Due to the compliance of the device, we must consider the relative movement of the pins. For the following tests, pin 3 was mechanically grounded by mounting it rigidly to the frame of the device so that the force and displacement output could be measured directly by measuring pin 1 (see Fig. 5). To measure the blocking force and the stiffness of the LPD, a probe mounted on the load cell was moved slowly back and forth against pin 1 in the w-direction while measuring the displacement of the top of the pin in the w-direction with the laser displacement meter. The probe was brought into contact with the pin with the DEA at rest. The DEA was then actuated at a constant 3.5 kV for the duration of the test.

Fig. 6 shows the resultant force and displacement. It can be seen that the peak blocking force, at zero displacement, is 94 mN, and that the free displacement, at zero force, is 0.61 mm. The force varies approximately linearly with displacement, with some hysteresis due to viscoelastic effects in the DEA membrane. Assuming a linear relationship, the pin stiffness is 153 mN/mm.

3.2. Bandwidth

To determine the bandwidth of the LPD, the displacement of the top of pin 1 in the w-direction was measured using the laser displacement meter while driving the DEA with sinusoidal inputs of different frequencies. For this experiment, no pins were grounded. The amplitude response for frequencies between 0.1 Hz and 100 Hz was measured. We

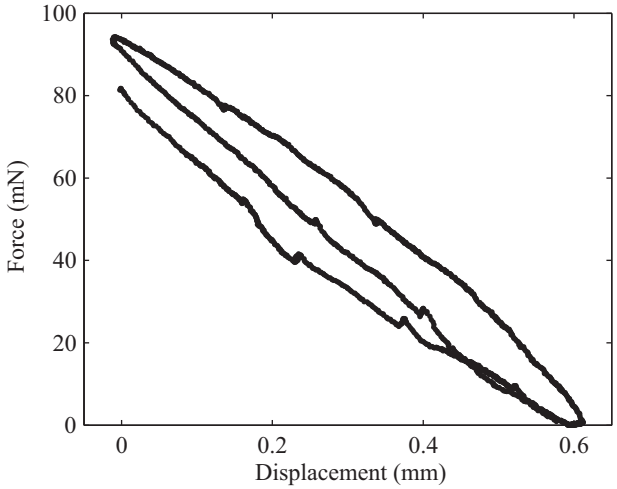

Figure 6. Force:displacement relationship of pin 1. The DEA was actuated at 3.5 kV, and pin 3 was mechanically grounded.

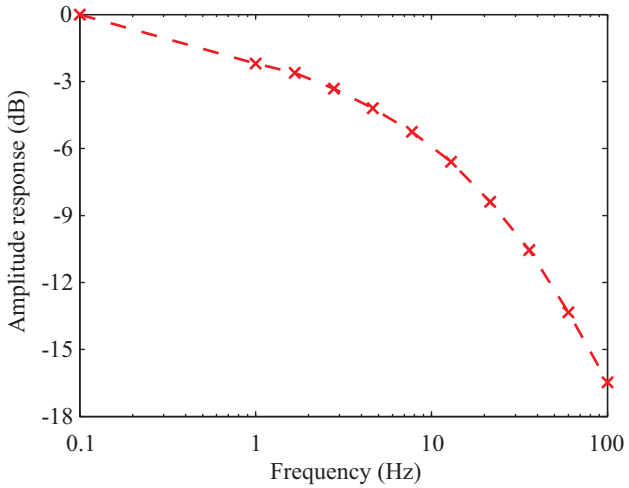

Figure 7. Bandwidth of LPD, with data points shown as crosses. We have taken 0 dB to be the response at 0.1 Hz.

have taken 0 dB to be the displacement amplitude at 0.1 Hz. Fig. 7 shows the resulting frequency response.

It is seen that there is significant roll-off in the amplitude response above ∼10 Hz. Between 0.1 and 10 Hz there is a 6 dB decrease in amplitude, likely to be due to the viscosity of the DEA membrane. This suggests that the LPD is well suited for stimulation of the SA1 mechanoreceptors. In future designs, the high-frequency response could be improved by replacing the VHB dielectric with a less viscous PDMS dielectric.

3.3. Loaded and unloaded displacement

We carried out tests to determine the relationship between applied voltage and pin displacement both unloaded and with a finger resting on the LPD. For the loaded tests,

the finger was rested on the device and gently pressed down. Due to the compliance in the structure, resting the finger on the device inadvertently led to some movement of the pins. This meant that direct measurement of pin displacement with a laser displacement meter was not meaningful.

Instead, optical tracking was used whereby cameras were positioned to view the LPD from the side (Fig. 5: direction u) and from below (Fig. 5: direction v) and videos were recorded of the experiments. Custom tracking software using digital image correlation was used to estimate the movement of the pins from the videos. From the side view, it was found that the compliant hinge could be modelled as a spherical joint (i.e. the hinge did not undergo significant lateral deformation), so that the displacement of the top of the pins could be inferred by tracking the bottom of the pins. To calibrate the image tracking software, the unloaded displacement of a single pin along direction w was measured with the laser displacement meter simultaneously to tracking the pins from the video.

The data from the loaded experiment was very noisy, with movements of the finger resulting in translation in the x-y-plane as well as rotation about the z-axis of all 4 pins together, so we required a noise-invariant feature to track. Each pin was therefore tracked separately, and the area of the polygon enclosed by the pins (i.e. the area of the stimulated skin) was computed. This area has been labelled A in Fig. 5. From the area, the relative area strain ε was calculated as $\varepsilon = A/A_0$, where A_0 is the area when the device is at rest. This feature was found to be very robust to noise.

For these experiments, the DEA voltage was ramped up in steps, with the voltage applied for 4 seconds and with 0 V applied for 4 seconds between steps (0.125 Hz). The videos were tracked continuously, with the displacement at the end of each step being used. For a dynamic tactile display, we consider 0.125 Hz to be approximately DC.

Fig. 8 shows the relative area strain against applied voltage for the loaded and unloaded cases. It can be seen that the strain is somewhat decreased in the loaded case. At the peak voltage of 3.5 kV, the unloaded relative area strain is -0.32, compared to -0.20 under load. A Piecewise Cubic Hermite Interpolating Polynomial (PCHIP) has been used to interpolate between the data points. It can be seen that for small strains the response is approximately quadratic with voltage as would be expected from (1). For larger strains, the response trails off which can be explained by nonlinear stiffness in the device as well as in the fingertip.

From the area enclosed between the pins, we can compute the mean pin displacement δ as the displacement each pin would undergo in the absence of noise to create the same relative area strain. Assuming small displacements, we can show that for 4 pins arranged in a square the relationship is

$$\delta = \frac{\sqrt{A_0} - \sqrt{A}}{\sqrt{2}}, \tag{2}$$

where δ is the mean pin displacement.

The mean pin displacement is shown in Fig. 9, from the same data used in Fig. 8. The interpolating curve was found by combining the interpolating curve from before

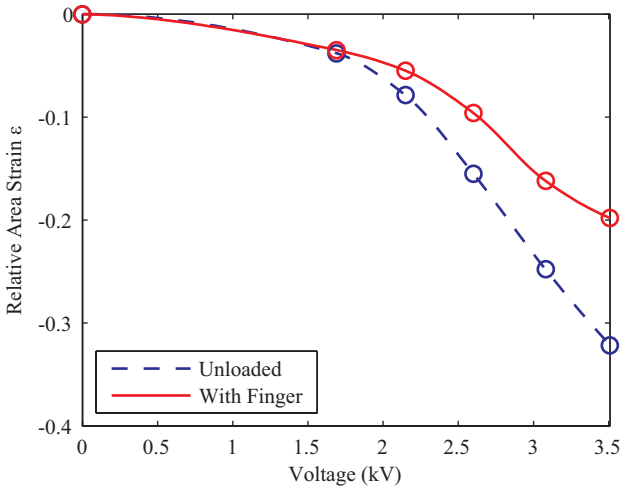

Figure 8. Characterisation of the relative area strain between the pins against applied voltage, in the unloaded case as well as with a finger resting on the LPD. Data points are shown as circles, with PCHIP interpolation between the data points.

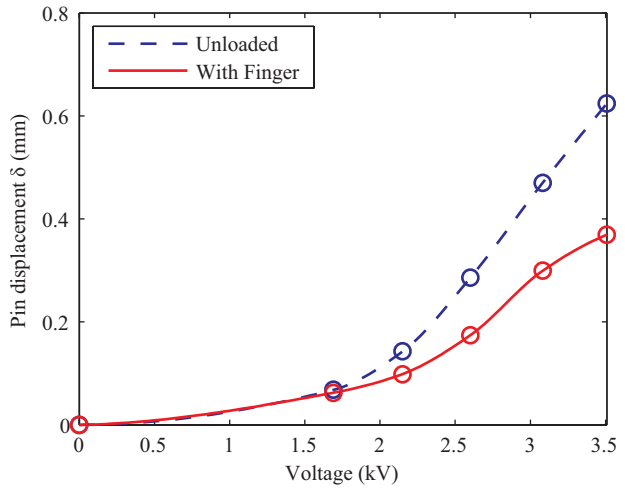

Figure 9. Mean displacement of the top of each pin, δ, computed from the area enclosed by the pins in order to eliminate noise.

with the relationship between ε and δ. It can be seen that at 3.5 kV, the unloaded displacement is 0.62 mm compared to 0.37 mm in the loaded case.

Fig. 10 shows the estimated pin displacement over time, together with the applied driving voltage.

3.4. Psychophysical study

Having characterised the mechanical properties of the LPD, we need to evaluate its effectiveness for creating tactile sensations to the user. Psychophysics is the study of the relationship between physical stimuli and a resulting sensation.

We designed an experiment to find the absolute sensitivity threshold at different

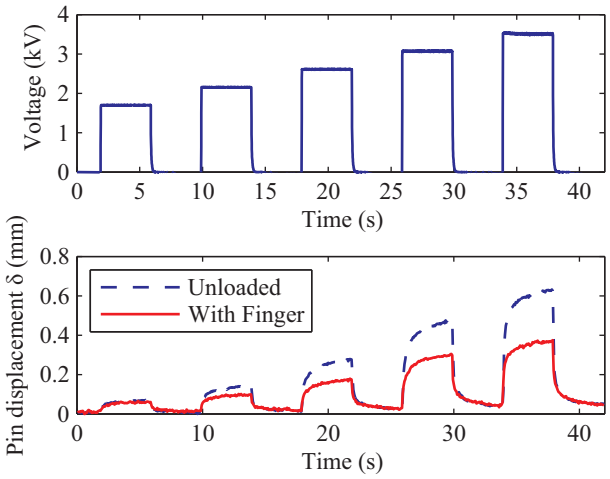

Figure 10. Mean displacement of single pin δ over time, computed from the area enclosed by the four pins.

frequencies. We considered frequencies between 1–100 Hz. For each frequency, subjects were presented with a sequence of trial stimuli, each with a duration of 1 s, with random intervals of 1–5 s between trials. Subjects were told to press a button when they could feel a stimulus. Stimuli were sinusoidal, with a 1.87 kV bias voltage added to make the entire stimulus signal positive. We took 0 dB to correspond to 2.25 kV peak-to-peak (pk-pk), i.e. a 0 dB stimulus would be given by $V_{out} = 1.87 + 1.125\sin(\omega t)$ where V_{out} is the voltage in kV. This means that 0 dB is close to the maximum output of the LPD.

We used a Quest adaptive psychometric algorithm [39], to generate the sequence of trials. After each trial, the maximum likelihood estimate of the sensitivity threshold is updated using the response of that trial and this is used to pick the amplitude of the following trial given some assumptions of the underlying psychometric function. Parameters in the Quest algorithm were set as suggested in [39] for a yes/no experiment. The initial guess of the threshold was taken as -10 dB, and sequences were terminated when the standard deviation of the threshold estimate was less than 0.1 dB and after a minimum of 15 trials.

We carried out the set of experiments on 5 volunteer subjects (4 male, 1 female). Subjects were sat at a desk with their preferred index finger resting on the LPD (Fig. 11), but were not given any instructions as to how to interact with the LPD (e.g. whether to rest the finger lightly or apply a normal force, and whether to have an open or closed hand). In this way, the results will better represent real interactions that people might have with the device.

The resulting sensitivity threshold as a function of the driving voltage is shown in Fig. 12. The mean sensitivity threshold is shown as a solid line, with error bars showing 1 standard deviation.

Taking into account the frequency response of the LPD (Fig. 7) and the voltage-displacement relationship (Fig. 9), we can estimate the pin displacement δ as a function

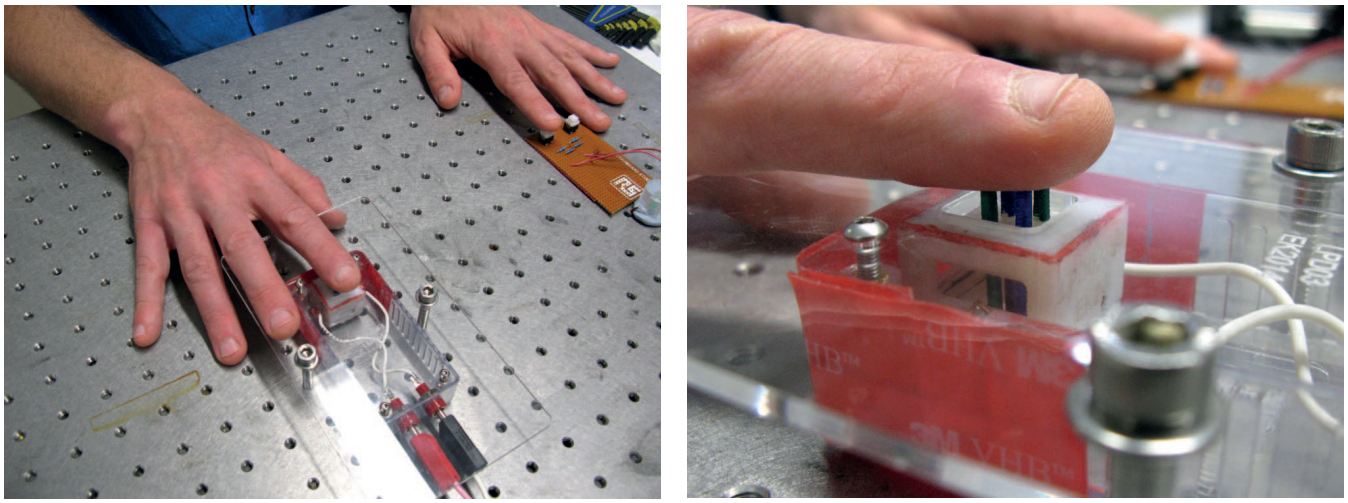

(a) **(b)**

Figure 11. The experimental setup for the psychophysical trials. Subjects were asked to place their preferred index finger on the device but were free to press hard/lightly and have the hand open/closed to create a more realistic scenario. (a): Overview. (b): close-up view of LPD.

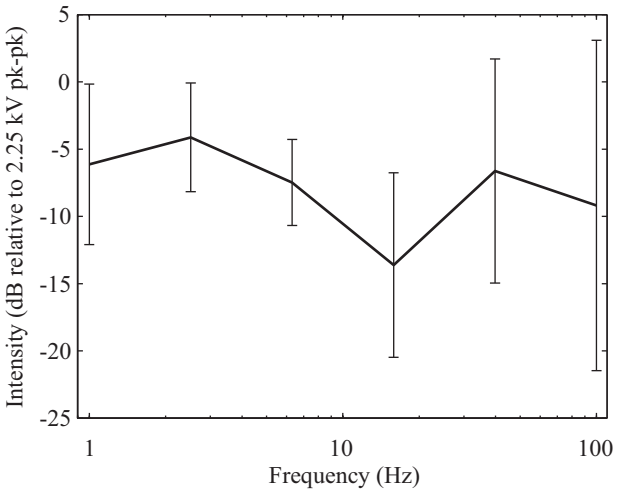

Figure 12. Mean absolute sensitivity threshold (dB relative to 2.25 kV pk-pk) from psychophysical study, for frequencies between 1–100 Hz. Error bars show 1 standard deviation.

of voltage V and frequency f, as

$$\delta(V, f) = G(f)\delta(V, 0) \tag{3}$$

where $G(f)$ is the frequency response and $\delta(V, 0)$ is the low-frequency voltage-displacement relationship. This allows us to compare the laterotactile sensitivity threshold to the sensitivity threshold for normal tactile stimulation. Bolanowski *et al* [3] found the absolute sensitivity threshold of the thenar eminence as a function of frequency, which is identical to the sensitivity of the fingertip [12].

Fig. 13 shows the estimated laterotactile absolute sensitivity threshold in dB relative

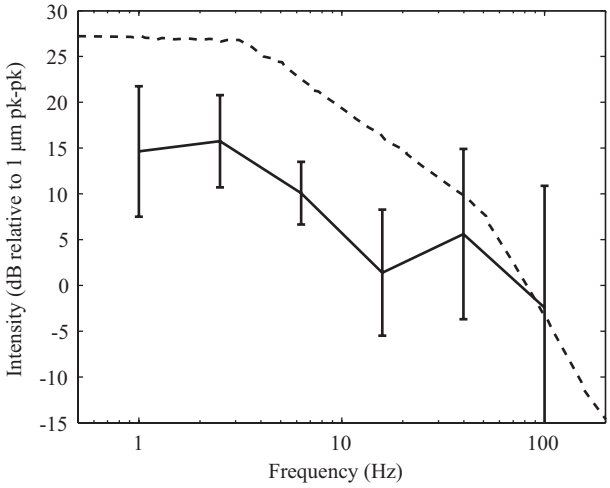

Figure 13. Mean absolute sensitivity threshold for displacement. The dashed line shows the sensitivity threshold for normal tactile stimulation, taken from [3]. It can be seen that for low frequencies humans are significantly more sensitive to laterotactile stimulation.

to 1 μm displacement, together with the normal sensitivity threshold from [3].

It can be seen that at low frequencies the sensitivity threshold is significantly lower for laterotactile sensations. At high frequencies, there appears to be little difference between the two modalities.

The FA1 and SA1 afferents (Fig. 1) are sensitive to frequencies up to $\sim$50 Hz [2]. From Fig. 13 it would appear that laterotactile stimulation is more effective in this range of frequencies. Thus, the hypothesis that laterotactile stimulation functions as shown in Fig. 1 (b) seems plausible.

These results show that laterotactile stimulation could be very well suited for tactile devices, in particular for lower frequency ranges.1

4. Discussion and conclusion

We have presented the design of a compliant laterotactile display, using a soft Dielectric Elastomer Actuator. The compliance in the actuator means that the device can move with the user's finger with little effect on the tactile information, which is essential for a comfortable wearable device. We have characterised a prototype of the display, including a basic psychophysical study demonstrating that the device can create strong tactile sensations over a wide range of frequencies.

We have demonstrated that with the manufacturing technique presented here displays with a spatial resolution of 2.5 mm can be created, which would allow for sophisticated tactile information to be conveyed. Performance of the display could be improved significantly if a more sophisticated multilayer actuator with a PDMS dielectric layer was used.

The design of the LPD could be scaled up to a large array of pins, actuated by a

single DEA membrane. However, compact high-voltage driving electronics suitable for driving a large array of DEAs have not yet been realised and further development is required in this area. This could be achieved with an array of high voltage amplifiers, or alternatively an array of high voltage switches together with a small number of high-voltage amplifiers.

Our prototype LPD has a rigid frame, but the design could be readily adapted to incorporate a soft and compliant frame since the DEA actuator is soft and there is inherent compliance in the device mechanism. The mechanism would also be applicable for devices using other actuators such as Shape Memory Alloys or pneumatic actuators.

It was observed that during the psychophysical tests the pins would be displaced substantially from involuntary movements of the fingertip, due to the compliance of the structure. However, the functionality of the tactile display was not noticeably affected by this movement. This demonstrates the effect of the passive compliance in the actuator; the display is able to move with and conform to the user with minimal effect on the produced tactile sensation.

Here we have considered tactile stimulation of the glabrous skin of the fingertip. Laterotactile stimulation could also be well suited for other devices such as a tactile wrist strap, however the different structure and innervation of the hairy skin mean that the requirements of spatial resolution and stimulation amplitude will be very different.

We are currently further investigating the psychophysics of laterotactile stimulation, including effects of pin spacing and also looking at laterotactile stimulation of hairy skin. This will allow for the design of more sophisticated wearable compliant tactile displays.

Acknowledgements

This work was supported with a PhD scholarship from the James Dyson Foundation.

References

[1] JG Linvill and JC Bliss. A direct translation reading aid for the blind. *Proc. IEEE*, 54(1), 1966.

[2] Roland S Johansson and J Randall Flanagan. Coding and use of tactile signals from the fingertips in object manipulation tasks. *Nature reviews. Neuroscience*, 10(5):345–59, May 2009.

[3] Stanley J Bolanowski, George A Gescheider, R T Verrillo, and C M Checkosky. Four channels mediate the mechanical aspects of touch. *The Journal of the Acoustical Society of America*, 84(5):1680–94, November 1988.

[4] Kenneth O Johnson. The roles and functions of cutaneous mechanoreceptors. *Current opinion in neurobiology*, 11(4):455–61, August 2001.

[5] Kenneth O Johnson and John R Phillips. Tactile spatial resolution. I. Two-point discrimination, gap detection, grating resolution, and letter recognition. *Journal of neurophysiology*, 46(6):1177–1192, 1981.

[6] Ryo Kikuuwe, Akihito Sano, Hiromi Mochiyama, Naoyuki Takesue, K. Tsunekawa, S. Suzuki, and Hideo Fujimoto. The Tactile Contact Lens. *Proc. IEEE Sensors*, pages 535–538, 2004.

[7] Vincent Hayward and Juan Manuel Cruz-Hernandez. Tactile display device using distributed lateral skin stretch. In *Symposium on Haptic Interfaces for Virtual Environment and Teleoperator Systems*, 2000.

[8] Vincent Hayward, Alexander V Terekhov, Sheng-Chao Wong, Pontus Geborek, Fredrik Bengtsson, and Henrik Jörntell. Spatio-temporal skin strain distributions evoke low variability spike responses in cuneate neurons. *J. R. Soc. Interface*, 11, 2014.

[9] K Kyung and D Kwon. Tactile displays with parallel mechanism. In *Parallel Manipulators, New Developments*. I-Tech Education and Publishing, 2008.

[10] Marc Matysek, Peter Lotz, and Helmut F. Schlaak. Tactile display with dielectric multilayer elastomer actuators. *Proc. SPIE*, 7287, March 2009.

[11] Calum Roke, Chris Melhuish, Tony Pipe, David Drury, and Craig Chorley. Deformation-based tactile feedback using a biologically-inspired sensor and a modified display. In *Towards Autonomous Robotic Systems*, pages 114–124. Springer Berlin Heidelberg, 2011.

[12] George a Gescheider, Stanley J Bolanowski, Jennifer V Pope, and Ronald T Verrillo. A four-channel analysis of the tactile sensitivity of the fingertip: frequency selectivity, spatial summation, and temporal summation. *Somatosensory & motor research*, 19(2):114–24, January 2002.

[13] Ryo Kikuuwe, Akihito Sano, Hiromi Mochiyama, Naoyuki Takesue, and Hideo Fujimoto. Enhancing haptic detection of surface undulation. *ACM Transactions on Applied Perception*, 2(1):46–67, January 2005.

[14] Qi Wang and Vincent Hayward. Biomechanically optimized distributed tactile transducer based on lateral skin deformation. *International Journal of Robotics Research*, 29(4):323–335, 2010.

[15] Gregory J. Gerling and Geb W. Thomas. The effect of fingertip microstructures on tactile edge perception. *EuroHaptics*, pages 63–72, 2005.

[16] Shinobu Kuroki, Hiroyuki Kajimoto, Hideaki Nii, Naoki Kawakami, and Susumu Tachi. Proposal of the Stretch Detection Hypothesis of the Meissner Corpuscle. *EuroHaptics*, pages 245–254, 2008.

[17] Silmon James Biggs and Mandayam A Srinivasan. Tangential Versus Normal Displacements of Skin: Relative Effectiveness for Producing Tactile Sensations. In *Proc. Haptics*, pages 121–128. IEEE, 2002.

[18] Knut Drewing, Michael Fritschi, Regine Zopf, Marc O Ernst, and Martin Buss. First evaluation of a novel tactile display exerting shear force via lateral displacement. *ACM Transactions on Applied Perception*, 2(2):118–131, 2005.

[19] Masashi Nakatani, Akihiro Sato, Susumu Tachi, and Vincent Hayward. Tactile illusion caused by tangential skin strain and analysis in terms of skin deformation. In *EuroHaptics*, pages 229–237, 2008.

[20] Vincent Lévesque and Vincent Hayward. Laterotactile rendering of vector graphics with the stroke pattern. In *Proc. EuroHaptics*, pages 25–30. Springer, 2010.

[21] Darwin G Caldwell, N G Tsagarakis, and C Giesler. An Integrated Tactile/Shear Feedback Array for Stimulation of Finger Mechanoreceptor. In *IEEE ICRA*, pages 287–292, 1999.

[22] Michael Fritschi, Martin Buss, Knut Drewing, Regine Zopf, and Marc O Ernst. Tactile Feedback Systems. *IEEE IROS*, pages 1–21, 2004.

[23] Robert F Shepherd, Filip Ilievski, Wonjae Choi, Stephen A Morin, Adam A Stokes, Aaron D Mazzeo, Xin Chen, Michael Wang, and George M. Whitesides. Multigait soft robot. *PNAS*, 108(51), 2011.

[24] Ronald E. Pelrine. High-speed electrically actuated elastomers with strain greater than 100%. *Science*, 287(5454):836–839, February 2000.

[25] Federico Carpi, Roy Kornbluh, Peter Sommer-Larsen, and Gursel Alici. Electroactive polymer actuators as artificial muscles: are they ready for bioinspired applications? *Bioinspiration & biomimetics*, 6(4):045006, December 2011.

[26] Kwangmok Jung, Kwang J. Kim, and Hyouk Ryeol Choi. A self-sensing dielectric elastomer actuator. *Sensors and Actuators A: Physical*, 143(2):343–351, May 2008.

[27] Hyouk Ryeol Choi, S W Lee, Kwangmok Jung, Ja Choon Koo, S I Lee, H G Choi, Jaewook Jeon, and Jae-Do Nam. Tactile Display as a Braille Display for the Visually Disabled. In *IEEE IROS*,

pages 1985–1990, 2004.

[28] Ig Mo Koo, Kwangmok Jung, Ja Choon Koo, Jae-do Nam, Young Kwan Lee, and Hyouk Ryeol Choi. Development of soft-actuator-based wearable tactile display. *IEEE Transactions on Robotics*, 24(3):549–558, June 2008.

[29] Noel Runyan and Deane Blazie. EAP actuators aid the quest for the "Holy Braille" of tactile displays. *Proc. SPIE*, 7642, March 2010.

[30] Yoseph Bar-Cohen. Refreshable Braille displays using EAP actuators. *Proc. SPIE*, 7642, March 2010.

[31] Marc Matysek, Peter Lotz, Klaus Flittner, and Helmut F. Schlaak. Vibrotactile display for mobile applications based on dielectric elastomer stack actuators. *Proc. SPIE*, 7642, March 2010.

[32] Federico Carpi, Gabriele Frediani, and Danilo De Rossi. Hydrostatically coupled dielectric elastomer actuators for tactile displays and cutaneous stimulators. *Proc. SPIE*, 7642, March 2010.

[33] P. Chakraborti, H.a. Karahan Toprakci, P. Yang, N. Di Spigna, P. Franzon, and T. Ghosh. A compact dielectric elastomer tubular actuator for refreshable Braille displays. *Sensors and Actuators A: Physical*, 179:151–157, June 2012.

[34] Hyung Seok Lee, Dong Hyuk Lee, Dea Gyeong Kim, Ui Kyum Kim, Choong Han Lee, Nguyen Ngoc Linh, Nguyen Canh Toan, Ja Choon Koo, Hyungpil Moon, Jae-do Nam, Jeongheon Han, and Hyouk Ryeol Choi. Tactile display with rigid coupling. *Proc. SPIE*, 8340, April 2012.

[35] Lars Espen Knoop and Jonathan Rossiter. Towards shear tactile displays with DEAs. In Yoseph Bar-Cohen, editor, *Proc. SPIE*, volume 9056. SPIE, 2014.

[36] Andrew T Conn and Jonathan Rossiter. Antagonistic dielectric elastomer actuator for biologically-inspired robotics. *Proc. SPIE*, 7976, March 2011.

[37] Andrew T Conn and Jonathan Rossiter. Towards holonomic electro-elastomer actuators with six degrees of freedom. *Smart Materials and Structures*, 21(3), March 2012.

[38] Jonathan Rossiter, Peter Walters, and Boyko Stoimenov. Printing 3D dielectric elastomer actuators for soft robotics. *Proc. SPIE*, 7287, March 2009.

[39] Andrew B Watson and Denis G Pelli. QUEST: A Bayesian adaptive psychometric method. *Perception & psychophysics*, 33(2):113–120, 1983.